Case Reports in Dermatology

Case Rep Dermatol 2015;7:1–6

DOI: 10.1159/000371732
Published online: January 14, 2015

1662–6567/15/0071–0001$39.50/0
www.karger.com/cde

Karger Open access

Merkel Cell Carcinoma Concomitant with Invasive Bowen's Disease: Immunohistochemical Investigation of Tumor-Infiltrating Leukocytes

Hisayuki Tono Taku Fujimura Eimei Iwama Yoshiyuki Kusakari
Sadanori Furudate Yumi Kambayashi Takahiro Haga Akira Hashimoto
Setsuya Aiba

Department of Dermatology, Tohoku University Graduate School of Medicine, Sendai, Japan

Key Words
Invasive Bowen's disease · Merkel cell carcinoma · Tumor-infiltrating leukocytes · CD8 · Caspase 3

Abstract
Merkel cell carcinoma (MCC) is an aggressive, cutaneous, neuroendocrine carcinoma and, in rare cases, occurs with Bowen's disease (BD). In this report, we describe a case of MCC concurrent with invasive BD and compare the profiles of tumor-infiltrating leukocytes in the lesional skin of MCC and invasive BD. Interestingly, immunohistochemical study revealed significant numbers of CD8+ cells and caspase 3-expressing cells in the same areas of invasive BD and MCC. Our present case suggests that MCC concurrent with invasive BD might have a good prognosis because of the substantial number of CD8+ cells in the tumor.

Introduction

Merkel cell carcinoma (MCC) is an aggressive, cutaneous, neuroendocrine carcinoma that originates from either Merkel cells or from pluripotent stem cells in the basal layer of the epidermis [1, 2]. Recent reports suggested that the type of tumor-infiltrating leukocytes (TILs) could determine the prognosis and tumor-specific survival of MCC [3–5]. Bowen's disease (BD) is defined as carcinoma in situ; the tumor shows atypical pleomorphism, cell

KARGER 125 YEARS

Taku Fujimura
Department of Dermatology
Tohoku University Graduate School of Medicine
Seiryo-machi 1-1, Aoba-ku, Sendai 980-8574 (Japan)
E-Mail tfujimura1@mac.com

clumping, irregular mitosis and individual cell keratinization. BD progresses to invasive BD, with the cytological characteristics of BD [6]. In addition, as we previously reported, both invasive and non-invasive BD contain substantial numbers of TILs, including CD8+ cells, Foxp3+ regulatory T cells (Tregs) and CD163+ macrophages [7]. Although several cases of MCC concurrent with BD have already been reported [8, 9], there has been no English language report investigating TILs in MCC with BD. In this report, we describe a case of MCC concurrent with invasive BD and compare the profiles of TILs in the lesional skin of MCC and invasive BD.

Case Report

A 71-year-old Japanese male visited our outpatient clinic with a 6-month history of a rapidly growing red plaque on his back. On his initial visit, physical examination revealed a red, pigmented plaque, 90 × 80 mm, with a dome-shaped elastic-soft nodule (fig. 1a). The diameter of the nodule was approximately 20 mm. A skin biopsy from the edge of the plaque revealed atypical squamous cells containing large oval nuclei with occasional conspicuous nucleoli, with individual keratinization, mitotic figures and clumping cells. In addition, the biopsy specimen from the center of the nodule revealed dense infiltrating atypical squamous cells throughout the dermis (fig. 1c). We first diagnosed this patient as invasive BD and excised the tumor with a 5-mm margin. Unexpectedly the histological finding of the whole tumor revealed that the squamous cell-composed tumor was surrounded by another type of tumor composed of small round cells with scant cytoplasm and oval nuclei (fig. 1b, d). These small round cells were positive for AE1/AE3, cytokeratin 20, synaptophysin and CD56, and negative for 34βE12, cytokeratin 7, chromogranin A and TTF1. From the above findings, we diagnosed this tumor as MCC concomitant with invasive BD. We screened for a possible internal malignancy with positron emission tomography computed tomography and found no evidence of metastasis.

As we and other reports suggested [3, 4, 7], both invasive BD and MCC contain substantial numbers of immunoreactive and immunosuppressive cells. Notably, a previous report even suggested that the number of tumor-infiltrating CD8+ cells determines the prognosis of MCC [3]. Therefore, we further employed immunohistochemical staining for CD8 (fig. 2a, b), caspase 3 (fig. 2c, d), Foxp3 (fig. 3a, b), CD163 (fig. 3c, d) and CD206 (fig. 3e, f) in the lesional areas of invasive BD and MCC. Substantial numbers of immunoreactive and immunosuppressive cells were detected at the edge of the tumor in invasive BD, whereas TILs were scattered at the center of the tumor in MCC. Both invasive BD and MCC contained caspase 3-expressing cells in the CD8-infiltrated areas, which suggested induction of an anti-tumor immune response in the tumor microenvironment by CD8+ cytotoxic T cells.

Discussion

Previous reports suggested the importance of evaluating the tumor microenvironment in the lesional skin of MCC. Indeed, Paulson et al. [3] reported an association between the infiltration of intratumoral CD8+ lymphocytes and improved MCC-specific survival. More recently, Dowlatshahi et al. [4] reported that a subset of tumor-associated macrophages (TAMs) in MCC expressed PD-L1, which contributes to the exhaustion of CD8+ effector T cells in the tumor microenvironment. Indeed, Afanasiev et al. [10] reported that Merkel cell polyomavirus (MCPyV)-specific CD8 T cells were detected directly ex vivo from the

blood samples of patients with MCPyV-positive MCC. Interestingly, MCPyV-specific CD8 T cells and MCC-infiltrating lymphocytes expressed higher levels of therapeutically targetable PD-1 [10]. Notably, MCPyV contributes to the carcinogenesis of MCC [11]. From an immunological point of view, recent reports also suggested that the expression of B7-H molecules, including PD-L1, on TAMs and tolerogenic dendritic cells is regulated by Tregs, and that the induction of Tregs is mediated by TAMs by B7-H-related signaling [12]. In aggregate, these reports suggested the significance of crosstalk between Tregs and TAMs in the lesional skin of MCC, and these immunosuppressive cells might contribute to the exhaustion of MCC-specific CD8+ T cells to maintain an immunosuppressive tumor microenvironment.

Concerning BD, we previously reported that substantial numbers of CD8+ cells were detected adjacent to tumor cells, and that the expression of PD-L1 on tumor cells diminished in parallel with the progression of BD, which might recover the exhausted CD8+ effector T cells in the tumor microenvironment of invasive BD, like MCC [4, 7]. Notably, although several cases of MCC concurrent with BD have already been reported [8, 9], to our knowledge, there is no English language report suggesting a prognostic factor for this type of tumor. In this report, we describe a case of MCC concurrent with invasive BD and compare the profiles of TILs in the lesional skin of MCC and invasive BD. Interestingly, immunohistochemical study revealed that both invasive BD and MCC contained significant numbers of CD8+ cells in the tumor lesion. Although this area contained substantial number of Foxp3+ Tregs and CD163+ TAMs, caspase 3-expressing cells were scattered in the lesional skin of BD and MCC, which might suggest induction of an anti-tumor immune response in the tumor microenvironment of MCC and BD. Our present case suggests that MCC concurrent with invasive BD might have a good prognosis because of the substantial number of CD8+ cells in the tumor. Since we did not directly assess the suppressive functions of these infiltrating cells, further analysis of the mechanisms underlying this phenomenon could offer fundamental insights into the mechanisms of our case. To confirm this hypothesis, further studies will be necessary in the future.

References

▶1 Ferringer T, Rogers HC, Metcalf JS: Merkel cell carcinoma in situ. J Cutan Pathol 2005;32:162–165.
▶2 Van Keymeulen A, Mascre G, Youseff KK, Harel I, Michaux C, De Geest N, Szpalski C, Achouri Y, Bloch W, Hassan BA, Blanpain C: Epidermal progenitors give rise to Merkel cells during embryonic development and adult homeostasis. J Cell Biol 2009;187:91–100.
▶3 Paulson KG, Iyer JG, Tegeder AR, Thibodeau R, Schelter J, Koba S, Schrama D, Simonson WT, Lemos BD, Byrd DR, Koelle DM, Galloway DA, Leonard JH, Madeleine MM, Argenyi ZB, Disis ML, Becker JC, Cleary MA, Nghiem P: Transcriptome-wide studies of Merkel cell carcinoma and validation of intratumoral CD8+ lymphocyte invasion as an independent predictor of survival. J Clin Oncol 2011;29:1539–1546.
▶4 Dowlatshahi M, Huang V, Gehad AE, Jiang Y, Calarese A, Teague JE, Dorosario AA, Cheng J, Nghiem P, Schanbacher CF, Thakuria M, Schmults CD, Wang LC, Clark RA: Tumor-specific T cells in human Merkel cell carcinomas: a possible role for Tregs and T-cell exhaustion in reducing T-cell responses. J Invest Dermatol 2013;133:1879–1889.
▶5 Asgari MM, Sokil MM, Warton EM, Iyer J, Paulson KG, Nghiem P: Effect of host, tumor, diagnostic, and treatment variables on outcomes in a large cohort with Merkel cell carcinoma. JAMA Dermatol 2014;150:716–723.
▶6 Mii S, Amoh Y, Tanabe K, Kitasato H, Sato Y, Katsuoka K: Nestin expression in Bowen's disease and Bowen's carcinoma associated with human papillomavirus. Eur J Dermatol 2011;21:515–519.
▶7 Furudate S, Fujimura T, Kambayashi Y, Aiba S: Comparison of immunosuppressive cells and cytotoxic cells in invasive and non-invasive Bowen's disease. Acta Derm Venereol 2014;94:337–339.
▶8 Ishida M, Okabe H: Merkel cell carcinoma concurrent with Bowen's disease: two cases, one with an unusual immunophenotype. J Cutan Pathol 2013;40:839–843.
▶9 Sirikanjanapong S, Melamed J, Patel RR: Intraepidermal and dermal Merkel cell carcinoma with squamous cell carcinoma in situ: a case report with review of literature. J Cutan Pathol 2010;37:881–885.

▶10 Afanasiev OK, Yelistratova L, Miller N, Nagase K, Paulson K, Iyer JG, Ibrani D, Koelle DM, Nghiem P: Merkel polyomavirus-specific T cells fluctuate with Merkel cell carcinoma burden and express therapeutically targetable PD-1 and Tim-3 exhaustion markers. Clin Cancer Res 2013;19:5351–5360.
▶11 Feng H, Shuda M, Chang Y, Moore PS: Clonal integration of a polyomavirus in human Merkel cell carcinoma. Science 2008;319:1096–1100.
▶12 Fujimura T, Ring S, Umansky V, Mahnke K, Enk AH: Regulatory T cells stimulate B7-H1 expression in myeloid-derived suppressor cells in ret melanomas. J Invest Dermatol 2012;132:1239–1246.

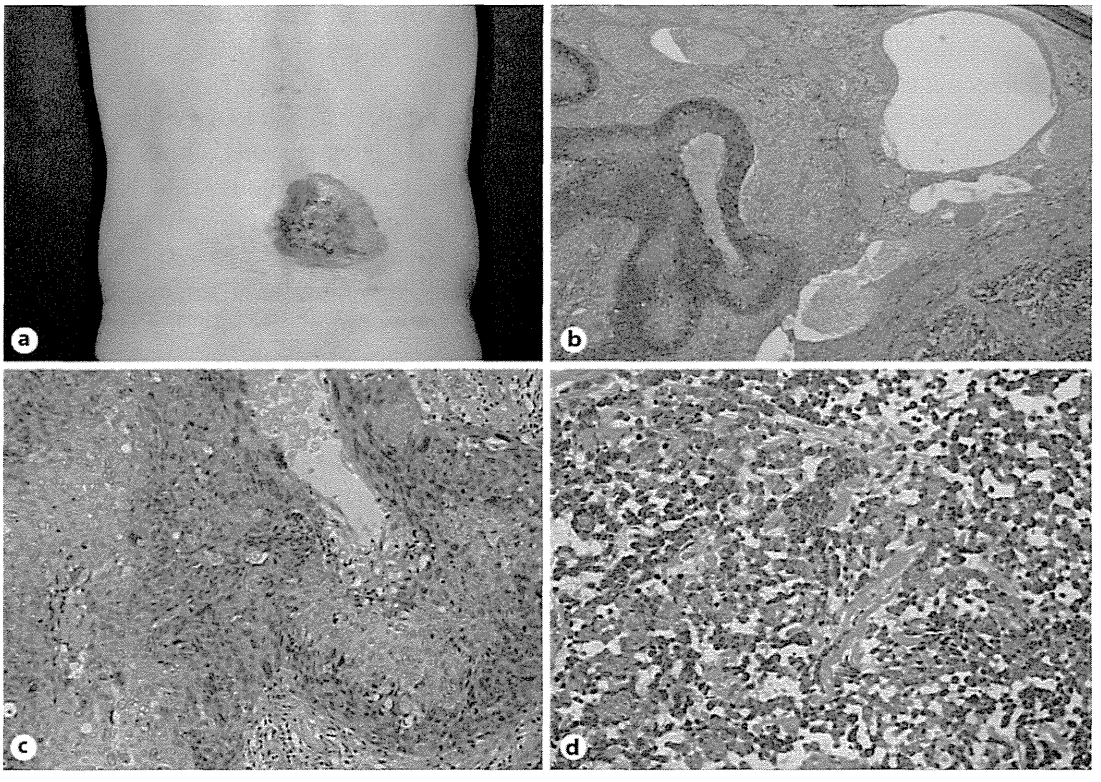

Fig. 1. **a** Red, pigmented plaque on the back, 90 × 80 mm, with a dome-shaped elastic-soft nodule. **b** The squamous cell-composed tumor was surrounded by another type of tumor. **c** Center of the tumor (squamous cell-composing tumor area): the atypical squamous cells contained large oval nuclei and occasionally conspicuous nucleoli, with individual keratinization, mitotic figures and clumping cells. **d** Peripheral areas of the tumor: small round cells with scant cytoplasm and oval nuclei. Original magnification: **b** ×50; **c**, **d** ×200.

Case Rep Dermatol 2015;7:1–6
DOI: 10.1159/000371732

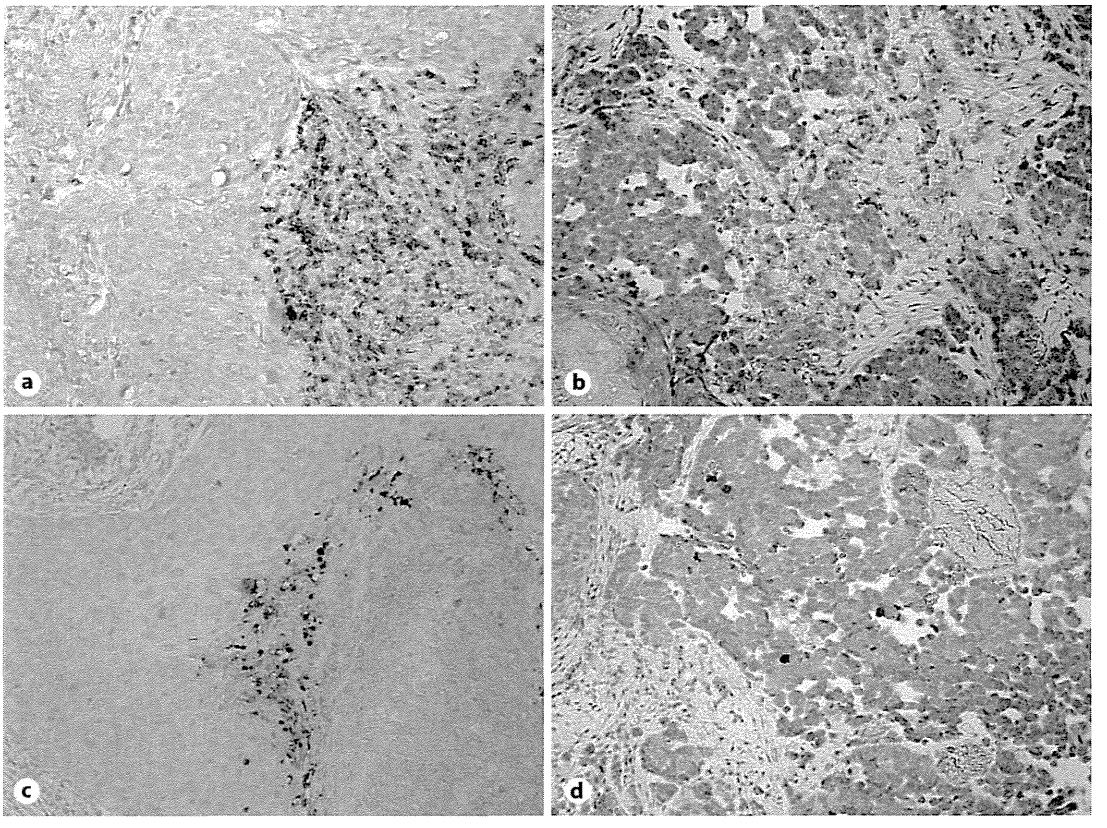

Fig. 2. CD8+ cells and caspase 3+ cells in the areas of invasive BD and MCC. Paraffin-embedded tissue samples were deparaffinized and stained with anti-CD8 antibody (**a**, **b**) and anti-caspase 3 antibody (**c**, **d**) for the areas of invasive BD (**a**, **c**) and MCC (**b**, **d**). The sections were developed with liquid permanent red. Original magnification: ×200.

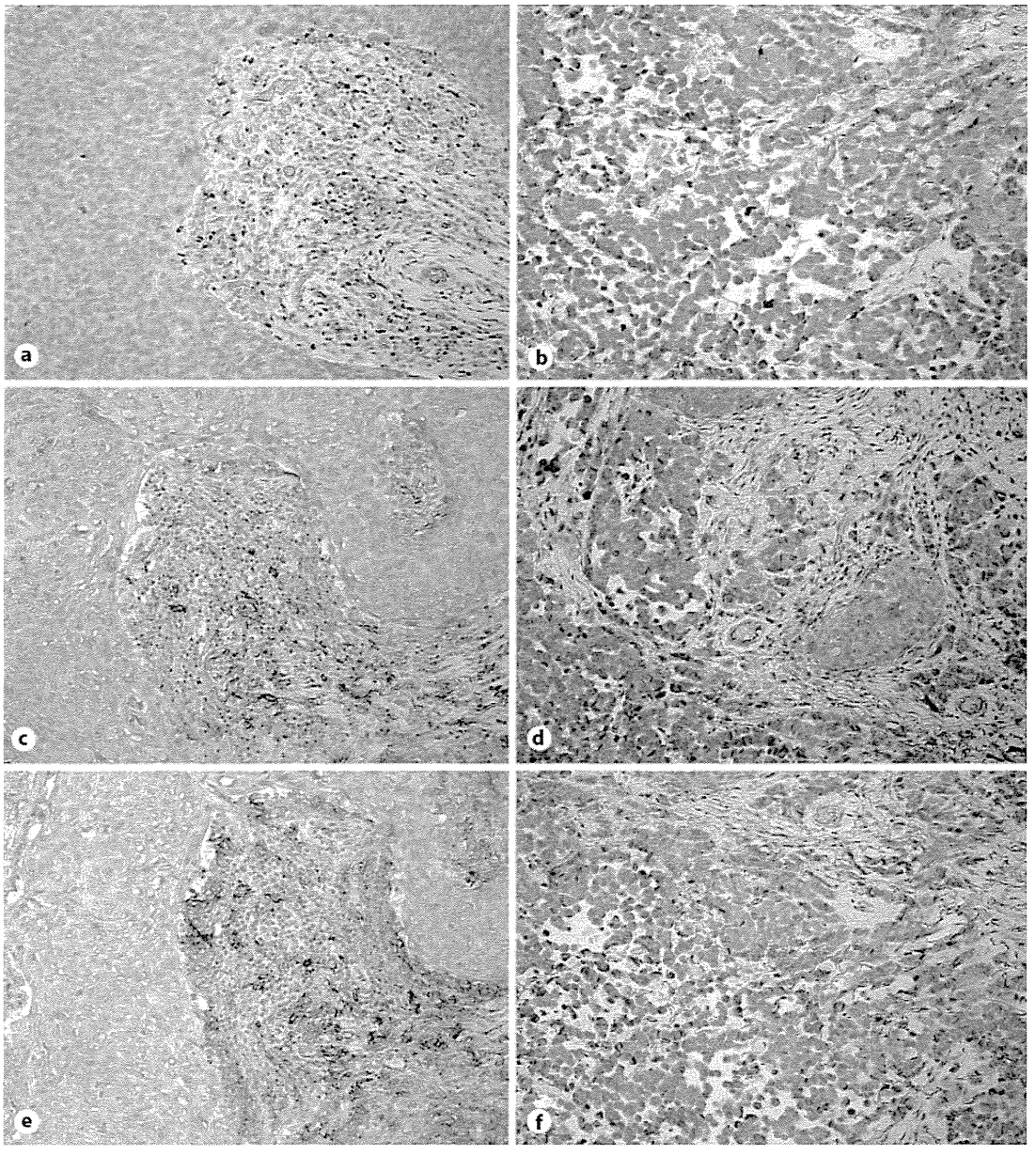

Fig. 3. Foxp3+ Tregs, CD163+ macrophages and CD206+ cells in the areas of invasive BD and MCC. Paraffin-embedded tissue samples were deparaffinized and stained with anti-Foxp3 antibody (**a**, **b**), anti-CD163 antibody (**c**, **d**) and anti-CD206 antibody (**e**, **f**) for the areas of invasive BD (**a**, **c**, **e**) and MCC (**b**, **d**, **f**). The sections were developed with liquid permanent red. Original magnification: ×200.

Original Paper

Dermatology

Dermatology 2015;230:250–255
DOI: 10.1159/000369166

Received: August 25, 2014
Accepted after revision: October 3, 2014
Published online: February 7, 2015

Immunomodulatory Effects of Peplomycin on Immunosuppressive and Cytotoxic Cells in the Lesional Skin of Cutaneous Squamous Cell Carcinoma

Taku Fujimura Yumi Kambayashi Sadanori Furudate Aya Kakizaki
Takahiro Haga Akira Hashimoto Setsuya Aiba

Department of Dermatology, Tohoku University Graduate School of Medicine, Sendai, Japan

Key Words
Squamous cell carcinoma · Peplomycin · Regulatory T cells · Cytotoxic T cells

Abstract
Background: Continuous intra-arterial administration of peplomycin (PEP) through a tumor-feeding artery using an intravascular indwelling catheter is one of the best treatments for cutaneous squamous cell carcinoma (SCC) on cosmetic areas. Although this reagent is useful for the treatment of SCC, its immunomodulatory effect on the tumor microenvironment is still unknown. ***Objective/Methods:*** In this study, we investigated the immunomodulatory effects of PEP on the tumor-infiltrating regulatory T cells and tumor-associated macrophages as well as $CD8^+TIA\text{-}1^+$ cytotoxic T cells in the lesional skin of 5 patients with SCC on the lips. ***Results:*** Our data suggest that, in addition to the direct antitumor effects, PEP decreased immunosuppressive cells and increased cytotoxic T lymphocytes at the tumor sites, which might maintain antitumor immune response against SCC.

Introduction

Cutaneous squamous cell carcinoma (SCC) is the second most common type of nonmelanoma skin cancer [1]. Concerning high-risk patients or tumors on cosmetic areas, the management of cutaneous SCC differs according to the case [1, 2]. Among the therapeutic options, chemotherapy is used for the treatment of inoperable cutaneous SCC. Indeed, we previously reported the efficacy of continuous intra-arterial administration of peplomycin (PEP) through a feeding artery of the tumor using an intravascular indwelling catheter [3].

PEP is a bleomycin derivative antibiotic and its cytotoxicity toward mammalian cells is due to its ability to induce single- and double-strand DNA breaks by the induction of G1-phase-specific apoptosis [4, 5]. Though this reagent is useful for the treatment of SCC [3, 6–8], its effect on the tumor microenvironment of SCC is still unknown. As we previously reported, immunosuppressive cells, such as tumor-associated macrophages (TAMs) and regulatory T cells (Tregs), are dominant in the cancer stroma of cutaneous SCC [9]. Therefore, we hypothesized

KARGER 125

1018–8665/15/2303–0250$39.50/0

E-Mail karger@karger.com
www.karger.com/drm

Taku Fujimura
Department of Dermatology
Tohoku University Graduate School of Medicine
Seiryo-machi 1-1, Aoba-ku, Sendai 980-8574 (Japan)
E-Mail tfujimura1@mac.com

that PEP might possess immunomodulatory effects on the cancer stroma of cutaneous SCC. In this report, we evaluated the immunomodulatory effects of intra-arterial administration of PEP on cutaneous SCC using immunohistochemical staining for $CD4^+CD25^+Foxp3^+$ Tregs and $CD68^+$ TAMs, as well as $CD8^+TIA\text{-}1^+$ tumor-infiltrating lymphocytes (TILs).

Materials and Methods

Reagents

We used the following antibodies (Abs) for immunohistochemical staining: anti-human CD4 Abs (Nichirei Co., Tokyo, Japan); anti-human CD8 (Dako, Kyoto, Japan), CD25 (Vector, Burlingame, Calif., USA), CD68 (Dako), Foxp3 (Abcam, Tokyo, Japan), and anti-TIA-1 Ab (Abcam). Mouse immunoglobulin (Ig) G2a, IgG2b and IgG1 isotype controls were obtained from R&D Systems (Minneapolis, Minn., USA).

Tissue Samples and Immunohistochemical Staining

We surgically excised tissue samples of stage II or stage III SCC on the lips before and after intra-arterial administration of 5 mg PEP once a day for 7–10 days in 5 cases treated in the Department of Dermatology at Tohoku University Graduate School of Medicine. The continuous intra-arterial administration of PEP through a superficial temporal artery decreased the mass of SCC within 6 weeks in all cases. There has been no sign of local recurrence or systemic lesions for at least 12 months for all cases. The study was approved by the ethics committee of Tohoku University Graduate School of Medicine, Sendai, Japan. All patients gave informed consent. All samples were processed for staining of CD4, CD8, CD68, CD163 and TIA-1 and developed with liquid permanent red (Dako A/S, Glostrup, Denmark) or with 3,3′-diaminobenzidine tetrahydrochloride (Wako Pure Chemical Industries, Osaka, Japan) as we previously reported [9]. Double staining of Foxp3 and CD4 or CD25 was performed as described previously [10]. Briefly, formalin-fixed paraffin-embedded tissue samples were sectioned at 4 μm and deparaffinized. After autoclaving for antigen retrieval treatment, the sections were blocked with goat serum for 10 min and exposed to primary Abs at 4°C overnight. Ab binding was demonstrated via alkaline phosphatase-conjugated anti-rabbit Ig [Histofine SAB-AP(R) kit; Nichirei] for anti-Foxp3 Ab or Ig from an unimmunized rabbit, and via peroxidase-conjugated anti-mouse Ig [Histofine SAB-PO(M) kits; Nichirei] for anti-CD25 Abs, or their isotype controls. Anti-Foxp3 Ab was developed with new fuchsin (Nichirei), whereas anti-CD25 Ab was visualized with 3,3′-diaminobenzidine tetrahydrochloride.

Assessment of Immunohistochemical Staining

Staining of infiltrated lymphocytes was examined in more than 5 random, representative fields from each section. The number of immunoreactive cells was counted using an ocular grid of 1 cm^2 at a magnification of ×400. The percentages of each cell fraction were defined as the numbers of each cell type per total numbers of lymphocytes (CD4 + CD8 + CD68). Data are expressed as the mean ± SD for Treg fractions in each skin disorder.

Color version available online

Fig. 1. Representative figures for case 1. **a** Cutaneous SCC on the lip. **b** After the continuous, intra-arterial administration of 5 mg PEP per day for 9 days, the tumor mass had rapidly regressed, leaving a scar.

Statistical Analysis

For a single comparison of two groups, Student's t test was used. The level of significance was set at $p = 0.05$.

Results

Administration of PEP Enhanced Lymphocyte Infiltration within SCC on the Lip

In all 5 cases, the tumors were reduced in size by intra-arterial administration of PEP (representative figures of case 1: fig. 1). Six weeks after the administration of PEP, we excised the remaining tumors and examined them histologically to identify the tissue responses to PEP. First we immunohistochemically characterized the infiltrated cells before and after the intra-arterial administration of PEP. Substantial numbers of TILs expressed CD4 with

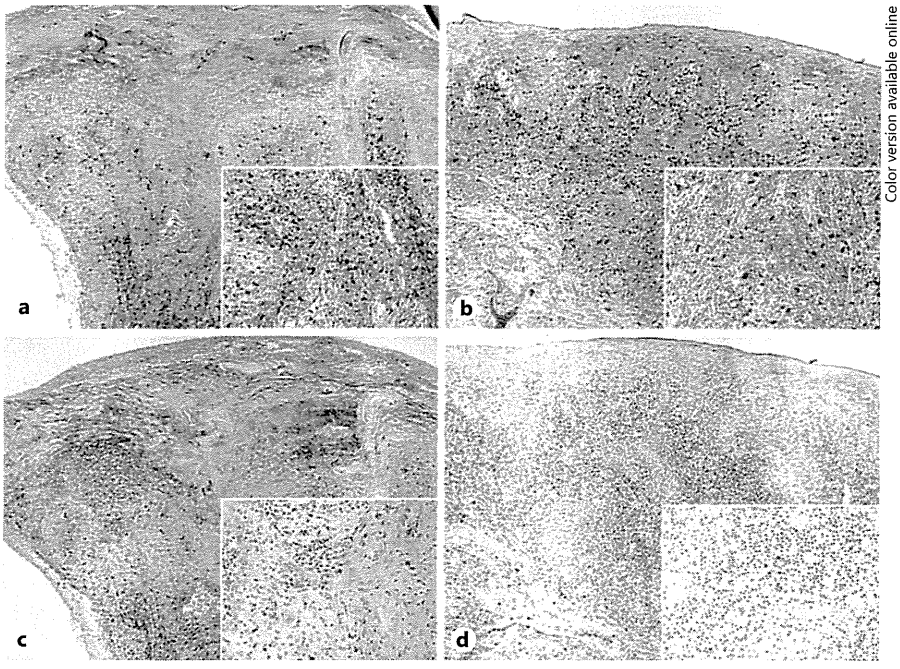

Color version available online

Fig. 2. Paraffin-embedded tissue samples from patients with SCC on the lip before (**a**, **c**) and after (**b**, **d**) the administration of PEP were deparaffinized and double-stained using a combination of the anti-Foxp3 Ab and an anti-CD25 Ab (**a**, **b**) or single-stained using the anti-CD68 Ab (**c**, **d**). Sections were developed with new fuchsin for Foxp3 (red) and with 3,3′-diaminobenzidine tetrahydrochloride for CD25 (brown), or developed with liquid permanent red for CD68. Original magnification: main ×50; inset ×400.

Table 1. Summary of the number and ratio of $CD4^+$, $CD8^+$, $CD68^+$, TIA-1^+ or $Foxp3^+$ cells in each case before and after the administration of PEP

	CD4	CD8	CD68	TIA-1	Foxp3	%CD4	%CD8	%CD68	%TIA-1	%Foxp3	Foxp3/CD4
Profiles of TILs before the administration of PEP											
1	184	61	132	50	143	48.8	16.1	35.0	13.2	37.9	77.7
2	236	90	70	62	164	59.6	22.7	17.7	15.7	41.4	69.5
3	138	66	68	49	77	50.7	24.3	25.0	18.0	28.3	55.8
4	209	26	52	14	167	72.8	9.1	18.1	4.8	58.2	79.9
5	208	85	67	47	101	57.8	23.6	18.6	13.1	36.7	63.5
Profiles of TILs after the administration of PEP											
1	348	376	27	554	83	46.3	50.0	3.6	73.8	11.0	23.9
2	271	372	21	264	75	40.8	56.0	3.2	39.8	11.3	27.7
3	149	110	5	167	31	56.4	41.7	1.9	63.3	11.7	20.8
4	141	193	15	152	30	40.0	55.1	4.6	43.4	8.6	21.2
5	190	144	18	176	30	54.0	40.9	5.1	50.0	8.5	15.8

%CD4 = CD/CD4 + CD8 + CD68; %CD8 = CD8/CD4 + CD8 + CD68; %CD68 = CD68/CD4 + CD8 + CD68; %TIA-1 = TIA-1/CD + CD8 + CD68; %Foxp3 = Foxp3/CD4 + CD8 + CD68.

Foxp3, CD25 with Foxp3 (fig. 2a) and CD68 (fig. 2c), suggesting that immunosuppressive Tregs and TAMs infiltrated into the SCC. Moreover, immunohistochemical staining for SCC after the administration of PEP (fig. 2b, d) revealed that it significantly reduced the ratio of $CD25^+Foxp3^+$ Tregs and $CD68^+$ tumor-resident macrophages. The number and ratio of Tregs and CD68 are summarized in table 1 and figure 3.

We also detected numerous cells that expressed TIA-1^+ and $CD8^+$, suggesting the activation of cytotoxic T lymphocytes (CTLs) infiltrating into the SCC (fig. 4a, c). In contrast to immunosuppressive cells such as Tregs

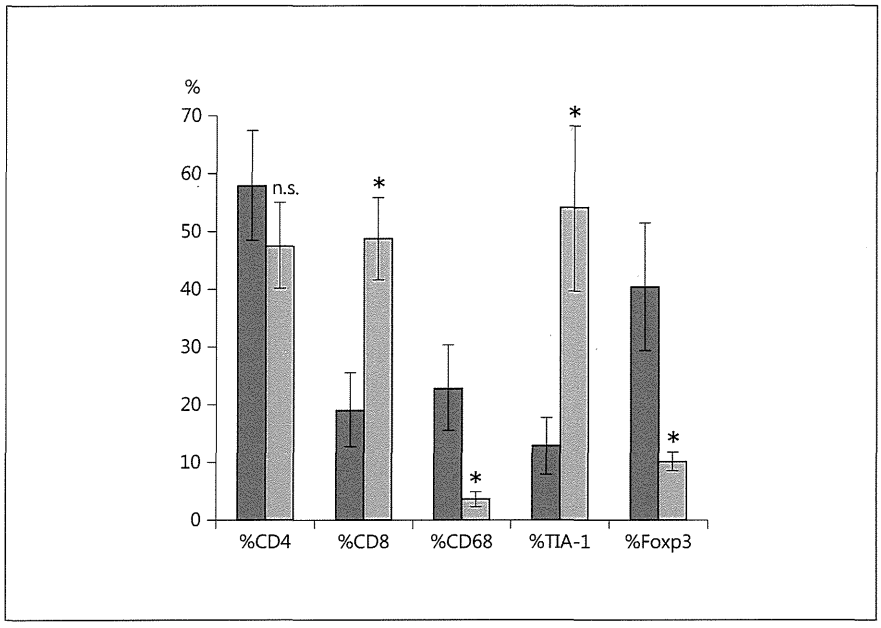

Fig. 3. Summary of the percentages of $CD4^+$, $CD8^+$, $CD68^+$, TIA-1^+ or $Foxp3^+$ cells among $CD4^+ + CD8^+ + CD68^+$ cells in lesional skin from patients with SCC. Five representative fields of each section were selected. The number of immunoreactive cells was counted using an ocular grid of 1 cm^2 at a magnification of ×400. The ratio of each cell type was defined as the ratio (%) of $CD4^+$, $CD8^+$, $CD68^+$, TIA-1^+ or $Foxp3^+$ cells to the total number of $CD4^+ + CD8^+ + CD68^+$ cells in each field, respectively. The data are expressed as the mean ± SD of each fraction. * $p < 0.05$.

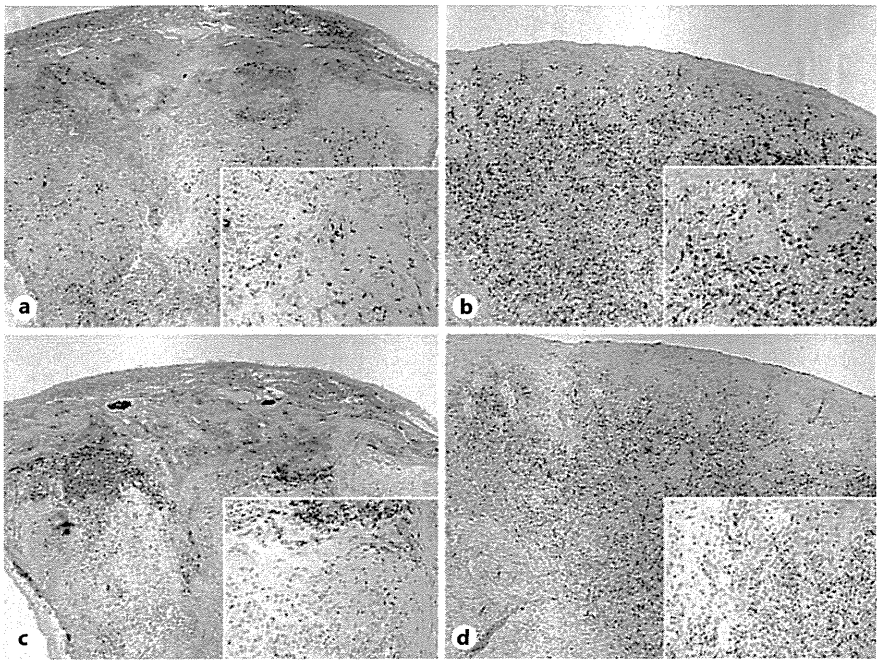

Color version available online

Fig. 4. Paraffin-embedded tissue samples from patients with SCC on the lip before (**a**, **c**) and after (**b**, **d**) the administration of PEP were deparaffinized and single-stained using the anti-CD8 Ab (**a**, **b**) or anti-TIA-1 Ab (**c**, **d**). Sections were developed with liquid permanent red. Original magnification: main ×50; inset ×400.

and TAMs, the administration of PEP significantly increased the ratio of TIA-1^+ and $CD8^+$ cells within the tumor (fig. 4b, d). This therapy did not have an effect on the ratio of $CD4^+$ cells. The number and ratio of CD4, CD8 and TIA-1 are summarized in table 1 and figure 3.

Discussion

In this report, we demonstrated that continuous intra-arterial administration of PEP through a facial artery using an intravascular indwelling catheter significantly decreased the ratio of $CD4^+CD25^+Foxp3^+$ Tregs and $CD68^+$

TAMs in the tumor, and significantly increased the ratio of $CD8^+TIA\text{-}1^+$ CTLs. These findings suggest that the effect of continuous intra-arterial administration of PEP is not only the direct cytotoxic effect on SCC, but might also induce an antitumor immune response by the decrease in Tregs and TAMs and increase in the effector T cells.

The induction of effector T cells, such as CTLs, has been a long-standing goal in cancer immunology and medical oncology. In this context, we previously reported that the intratumoral injection of an antitumor reagent, such as cationic liposome-encapsulated polyinosinic-polycytidylic acid and IFN-β, significantly increased the CTLs in melanoma [11, 12]. These data suggest that these reagents induce an antitumor effect against melanoma not only by killing the tumor but also by modulating the host immune systems at the tumor site. However, though we successfully induced CTLs by these reagents, there was no effect on the long-term survival of the melanoma-bearing host [11, 12]. This discrepancy may be explained by the recruitment of immunosuppressive cells, such as Tregs and TAMs, in the tumor microenvironment. Indeed, Mahnke et al. [13] reported that the depletion of Tregs in melanoma patients in vivo resulted in enhanced immune functions and the substantial development of antigen-specific $CD8^+$ T cells in vaccinated individuals. More recently, Telang et al. [14] assessed the efficacy of depleting Tregs in stage IV melanoma patients and concluded that the depletion of Tregs had a significant clinical effect in patients with unresectable stage IV melanoma. These reports suggested that depletion of Tregs could be an optimal supportive therapy for human skin tumor.

Recently, it was reported that Tregs in tumors not only suppressed effector T cells directly, but modified the phenotype of tumor-infiltrating macrophages to express inhibitory B7-H molecules and to produce IL-10 in both human and mouse models [15, 16]. We previously reported that depletion of Tregs significantly down-regulated the expression of immunosuppressive molecules, such as B7-H1, B7-H3 and B7-H4, on myeloid-derived suppressor cells (MDSCs) and reduced the tumor growth, indicating the concerted immunosuppressive activity of Treg and MDSCs [15]. MDSCs are a heterogeneous population of cells that promote an immunosuppressive environment in tumor-bearing hosts [17, 18]. In humans, MDSCs are a less defined and phenotypically heterogeneous group of cells that have only immunosuppressive activities in common [17, 18]. Interestingly, Tiemessen et al. [16] reported that $CD4^+CD25^+Foxp3^+$ Tregs produce IL-10, IL-4 and IL-13 and are able to steer monocyte differentiation toward alternative activated M2 macrophages. In addition, several reports also suggested the therapeutic effect of a selective reduction of MDSCs by chemotherapeutic drugs, such as gemcitabine or 5-fluorouracil [19, 20]. In aggregate, together with Tregs, immunosuppressive macrophages, such as MDSCs and TAMs, contribute to establishing the tumor microenvironment in skin cancer [17, 18, 21, 22], and the decrease in Tregs, MDSC or TAM could be an optimal supportive therapy for human skin tumor.

Concerning human SCC, recently several clinical reports suggested the contribution of tumor-infiltrating $Foxp3^+$ Tregs on the establishment and progression of the tumor [23–25]. In addition, Tabachnyk et al. [25] recently reported the immunomodulatory effect of neoadjuvant radiochemotherapy (i.v. administration of cisplatin and 5-fluorouracil with 50.4-Gy radiation) for oral SCC and suggested that the induction of cytotoxic T cells and a decrease in $Foxp3^+$ Tregs correlated with a better disease-free survival. They concluded that concurrent radiochemotherapy for oral SCC drives the composition of inflammatory cells in a prognostically favorable direction [25].

In addition to 2 previous cases of SCC on the ear successfully treated with intra-arterial administration of PEP [3], in this report, we described 5 cases of SCC on the lips successfully treated with intra-arterial administration of PEP through a superficial temporal artery. Notably, all of these 7 cases have achieved clinically complete remission. Moreover, we described the immunomodulatory effect of PEP on the TILs in cutaneous SCC. Since we did not directly assess the suppressive or effector function of these infiltrating cells in this study, further analysis of the mechanisms underlying this phenomenon could offer fundamental insights into the mechanisms of TILs in SCC. Such clarifications will need to be addressed in future investigations.

Acknowledgment

This study was supported in part by a grant-in-aid for scientific research from the Japan Society for the Promotion of Science (23791249 and 25461682). Role of sponsors: none.

Disclosure Statement

The authors make no financial disclosure and report no conflict of interests.

References

1 DeConti RC: Chemotherapy of squamous cell carcinoma of the skin. Semin Oncol 2012;39:145–149.

2 Lansbury L, Bath-Hextall F, Perkins W, Stanton W, Leonardi-Bee J: Interventions for non-metastatic squamous cell carcinoma of the skin: systematic review and pooled analysis of observational studies. BMJ 2013;347:f6153.

3 Haga T, Fujimura T, Takeuchi I, Deguchi M, Aiba S: Successful treatment of two cases of squamous cell carcinoma on the ear with intra-arterial administration of peplomycin through superficial temporal artery. Case Rep Dermatol 2014;6:207–212.

4 Okamura H, Morimoto H, Haneji T: Peplomycin-induced apoptosis in oral squamous cell carcinoma cells depends on bleomycin sensitivity. Oral Oncol 2001;37:379–385.

5 Chen HY, Zheng CY, Zou GL, Xie DX, Gong JP: Peplomycin induces G1-phase specific apoptosis in liver carcinoma cell line Bel-7402 involving G2-phase arrest. Acta Pharmacol Sin 2004;25:1698–1704.

6 Kirita T, Shimooka H, Yamanaka Y, Tatebayashi S, Yamamoto K, Nishimine M, Sugimura M: Prognostic value of response to preoperative chemoradiotherapy and residual tumor grades in tongue carcinoma. Oral Surg Oral Med Oral Pathol Oral Radiol Endod 2001;91:293–300.

7 Isobe K, Uno T, Hanazawa T, Kawakami H, Yamamoto S, Suzuki H, Iida Y, Ueno N, Okamoto Y, Ito H: Preoperative chemotherapy and radiation therapy for squamous cell carcinoma of the maxillary sinus. Jpn J Clin Oncol 2005;35:633–638.

8 Sugiyama T, Hasuo Y, Nishida T, Kamura T: Impact on survival following successful neoadjuvant chemotherapy and radical surgery for Stage IIb bulky and Stage IIIb cervical cancer. Gynecol Oncol 2001;81:330–331.

9 Kambayashi Y, Fujimura T, Aiba S: Comparison of immunosuppressive cells and immunomodulatory cells in keratoacanthoma and invasive squamous cell carcinoma. Acta Derm Venereol 2013;93:663–668.

10 Fujimura T, Okuyama R, Ito Y, Aiba S: Profiles of Foxp3+ regulatory T cells in eczematous dermatitis, psoriasis vulgaris and mycosis fungoides. Br J Dermatol 2008;158:1256–1263.

11 Fujimura T, Okuyama R, Ohtani T, Ito Y, Haga T, Hashimoto A, et al: Perilesional treatment of metastatic melanoma with interferon-beta. Clin Exp Dermatol 2009;34:793–799.

12 Fujimura T, Nakagawa S, Ohtani T, Ito Y, Aiba S: Inhibitory effect of the polyinosinic-polycytidylic acid/cationic liposome on the progression of murine B16F10 melanoma. Eur J Immunol 2006;36:3371–3380.

13 Mahnke K, Schönfeld K, Fondel S, Ring S, Karahanova S, Wiedemeyer K, Bedke T, Johnson TS, Storn V, Schallenberg S, Enk AH: Depletion of CD4+CD25+ human regulatory T cells in vivo: kinetics of Treg depletion and alteration in immune functions in vivo and in vitro. Int J Cancer 2007;120:2723–2733.

14 Telang S, Rasku MA, Clem AL, Carter K, Klarer AC, Badger WR, Milam RA, Rai SN, Pan J, Gragg H, Clem BF, McMasters KM, Miller DM, Chesney J: Phase II trial of the regulatory T cell-depleting agent, denileukin diftitox, in patients with unresectable stage IV melanoma. BMC Cancer 2011;11:515.

15 Fujimura T, Ring S, Umansky V, Mahnke K, Enk AH: Regulatory T cells (Treg) stimulate B7-H1 expression in myeloid-derived suppressor cells (MDSC) in *ret* melanomas. J Invest Dermatol 2012;132:1239–1246.

16 Tiemessen MM, Jagger AL, Evans HG, van Herwijnen MJC, John S, Taams LS: CD4+CD25+Foxp3+ regulatory T cells induce alternative activation of human monocytes/macrophages. Proc Natl Acad Sci USA 2007;104:19446–19451.

17 Fujimura T, Mahnke K, Enk AH: Myeloid derived suppressor cells and their role in tolerance induction in cancer. J Dermatol Sci 2010;59:1–6.

18 Gabrilovich DI, Nagaraj S: Myeloid-derived suppressor cells as regulators of the immune system. Nat Rev Immunol 2009;9:162–174.

19 Vincent J, Mignot G, Chalmin F, Ladoire S, Bruchard M, Chevriaux A, Martin F, Apetoh L, Rébé C, Ghiringhelli F: 5-Fluorouracil selectively kills tumor-associated myeloid derived suppressor cells resulting in enhanced T cell-dependent antitumor immunity. Cancer Res 2010;70:3052–3061.

20 Suzuki E, Kapoor V, Jassar AS, Kaiser LR, Albelda SM: Gemcitabine selectively eliminates splenic Gr-1+/CD11b+ myeloid suppressor cells in tumor-bearing animals and enhances antitumor immune activity. Clin Cancer Res 2005;11:6713–6721.

21 Pettersen JS, Fuentes-Duculan J, Suárez-Fariñas M, et al: Tumor-associated macrophages in the cutaneous SCC microenvironment are heterogeneously activated. J Invest Dermatol 2011;131:1322–1330.

22 Tjiu JW, Chen JS, Shun CT, Lin SJ, Liao YH, Chu CY, Tsai TF, Chiu HC, Dai YS, Inoue H, Yang PC, Kuo ML, Jee SH: Tumor-associated macrophage-induced invasion and angiogenesis of human basal cell carcinoma cells by cyclooxygenase-2 induction. J Invest Dermatol 2009;129:1016–1025.

23 Tallon B, Bhawan J: FoxP3 expression is increased in cutaneous squamous cell carcinoma with perineural invasion. J Cutan Pathol 2010;37:1184–1185.

24 Strauss L, Bergmann C, Gooding W, Johnson JT, Whiteside TL: The frequency and suppressor function of CD4+CD25highFoxp3+ T cells in the circulation of patients with squamous cell carcinoma of the head and neck. Clin Cancer Res 2007;13:6301–6311.

25 Tabachnyk M, Distel LV, Büttner M, Grabenbauer GG, Nkenke E, Fietkau R, Lubgan D: Radiochemotherapy induces a favourable tumour infiltrating inflammatory cell profile in head and neck cancer. Oral Oncol 2012;48:594–601.

Acta Derm Venereol 2015; 95: 822–825

CLINICAL REPORT

Retrospective Evaluation of Conservative Treatment for 140 Ingrown Toenails with a Novel Taping Procedure

Akiko WATABE, Kenshi YAMASAKI, Akira HASHIMOTO and Setsuya AIBA
Department of Dermatology, Tohoku University Graduate School of Medicine, Sendai, Japan

The aim of this study is retrospectively to review the efficacy of a taping procedure for treating ingrown toenails or for supporting other conservative treatments of ingrown toenails. A total of 140 ingrown toenails treated at the Dermatology Clinic in Tohoku University Hospital were retrospectively reviewed for demographic characteristics, association with granulation tissue or infection, treatment modalities and their outcomes, and classified according the treatment modalities. All the ingrown toenails were treated with a novel taping procedure, "slit tape-strap procedure" alone or in conjunction with other conservative treatments. The mean ± SD duration until pain relief and until cure of the ingrown toenail were 4.8 ± 4.7 days, range 0–24 and 21.0 ± 11.2 weeks, range 4–56, respectively. All of the treatments were all effective, although 18 cases recurred after treatment. The "slit tape-strap procedure" is effective in treating ingrown toenails, either as a monotherapy or as a supportive therapy for other conservative treatments. ***Key words: ingrowing nail; tape-strapping treatment; foot care; non-invasive conservative treatment.***

Accepted Feb 10, 2015; Epub ahead of print Feb 11, 2015

Acta Derm Venereol 2015; 95: 822–825.

Kenshi Yamasaki, Department of Dermatology, Tohoku University Graduate School of Medicine, 1-1 Seiryo-cho, Aoba-ku, Sendai 980-8574, Japan. E-mail: kyamasaki@med.tohoku.ac.jp

Ingrown toenails are a common condition seen by family physicians and hospital-based foot care units. The tip or edge of an ingrown toenail injures the skin of the nail fold and toe, causing pain, tenderness, infection, limited motion, and reduced quality of life. In patients with diabetes, injuries of the toes and foot often result in severe infections that can be life threatening. Invasive treatment for ingrown toenails may be contraindicated in patients with diabetes because of delayed wound healing.

There are 2 types of treatment for ingrown toenails: operative and conservative. Operative treatments are partial or complete nail avulsion, and matricectomy of ingrown nails by excision, bipolar diathermy, carbon dioxide laser or chemically with phenol, trichloroacetic acid and sodium hydroxide. Although operative treatments are effective and can achieve rapid resolution of infectious complications, such as excessive granulation tissue, the procedures are invasive, time-consuming and expensive, and may, result in relapse and deformity of the toenails (1).

Several conservative treatments are reported to reduce complications and achieve success in offices lacking surgical equipment. These methods include cotton-wool insertion under the corner of the nail and silver nitrate cautery of the granulation tissue (2), gutter treatment or flexible tube splinting (3–5), taping for embedded toenails (6), elastic wire device (7, 8), and a shape-memory alloy device (9). The goal of these conservative methods is: (*i*) to protect the nail fold from an ingrown toenail, and then (*ii*) to reform the transverse overcurvature of the ingrowing toenail. Since a few to several months are required for nail growth to reform the ingrown toenail, self-administered care for the nail fold and bed is essential for successful treatment of ingrowing toenails.

Among conservative treatments, taping is the safest, least painful and most convenient procedure. In addition, performed correctly and consistently, it can achieve its goal in mild cases (6). However, treating toenails that have caused the formation of granulation tissue or whose surrounding skin is sweaty can be difficult because the tape does not remain stuck to the skin. To compensate for this, we created a novel taping "slit tape-strap" procedure.

In our foot-care unit, we treated 140 ingrown toenails of 121 patients from October 2007 to July 2010. All patients were treated conservatively with the "split tape-strap" procedure. Among them, 48 ingrown toenails were treated with taping ("split tape-strap" alone or "split tape-strap" + "Nishioka's procedure"), while the other 92 ingrown toenails were treated with "split tape-strap" in conjunction with other conservative treatments. We retrospectively reviewed these cases and assessed the efficacy of the "slit tape-strap" procedure.

PATIENTS AND METHODS

Patients

This was a retrospective case study of ingrown toenails treated at the foot-care unit of the Dermatology Clinic in Tohoku University Hospital, Sendai, Japan, between October 2007 and July 2010. The study was approved by the ethics committee of Tohoku University Graduate School of Medicine. All patients were referred to the Dermatology Clinic and were treated with a taping procedure alone or in combination with other procedures, including an elastic wire device, gutter treatment, a shape-memory alloy device, or a combination of 2 or 3 different treatment devices.

To examine the background condition and to rule out possible adverse effects, some patients received examination for bacterial infection in the granulation tissue, or onychomycosis or fungal skin infection when necessary.

Data collection and classification

We systematically reviewed all case notes regarding 140 ingrown toenails of 121 patients. We collected information concerning gender, age, involved toes, nail shape, association with excessive granulation tissue, fungal or bacterial infection, applied treatments and their outcomes.

We classified the toenail shapes of the patients with ingrown toenails into 4 clinical types by modifying the classification reported by Baran et al. (10), since the ingrown toenails showed more or less transverse overcurvature. Clinical type 1 included the toenails with normal transverse curvature or overcurvature without rolling of the lateral plate margins. Clinical type 2 included pincer toenails that typically show the trumpet nail deformity with rolling of the lateral plate margins. Clinical type 3 included plicated toenails of moderate convexity with 1 or both lateral plate edges sharply bent to form a vertical sheet pressing into the lateral nail groove. Clinical type 4 included flat toenails without total loss of the transverse curve, mostly pressing into the lateral nail fold.

Treatment modality of the tape-strap method

We conducted 2 different taping procedures "split tape-strap procedure" and "Nishioka's procedure" by which the patients were taught how to cut and apply elastic tape to their ingrown nails. The tape was changed every 1 or 2 days.

The "split tape-strap procedure" was conducted as follows. Depending on the width and length of the toe, the elastic tape is cut into pieces 3 cm wide and 8–10 cm long and folded in half longitudinally (Fig. 1A). The slit, cut to the width of the ingrown nail, is made at one-third the length of the tape-strap from the short edge (Fig. 1B and 1C). To apply "split tape-strap procedure" to ingrown nails (Fig. 1D and 1E), the ingrown nail tip is set in the centre of the slit by orienting the shorter side of the tape toward the dorsal side of the toe, and the slit edge of the longer side of the tape is hooked on the ingrown nail (red arrows in Fig, 1F). The longer side of the tape-strap is then attached to the plantar side of the toe with tension to draw the distal nail-fold skin toward the plantar side (blue arrows in Fig. 1F and 1G). Under mild tension (black arrows in Fig. 1H), the shorter side of tape is attached to the dorsal side of the toe. The "slit tape-strap procedure" can be applied to any toe by choosing tape of the appropriate width for each toe (Fig. 1I).

In Nishioka's procedure, first introduced by Nishioka et al. (6) and modified by Arai et al. (5), an elastic strip of tape is cut to approximately 15–20 mm wide and 5 cm long and applied so that it allows the lateral nail fold to be pulled away from the toenail. This is usually done in an oblique and proximal direction over the pulp of the toe without impairing the joint movement and avoiding a circular constriction of the toe. A second, so-called anchor tape, is applied over the beginning of the first tape to fix it and exert more pull on the distal nail fold. In this study, we first applied the "split tape-strap procedure" and then conducted Nishioka's procedure to utilize "split tape-strap" as an anchor tape.

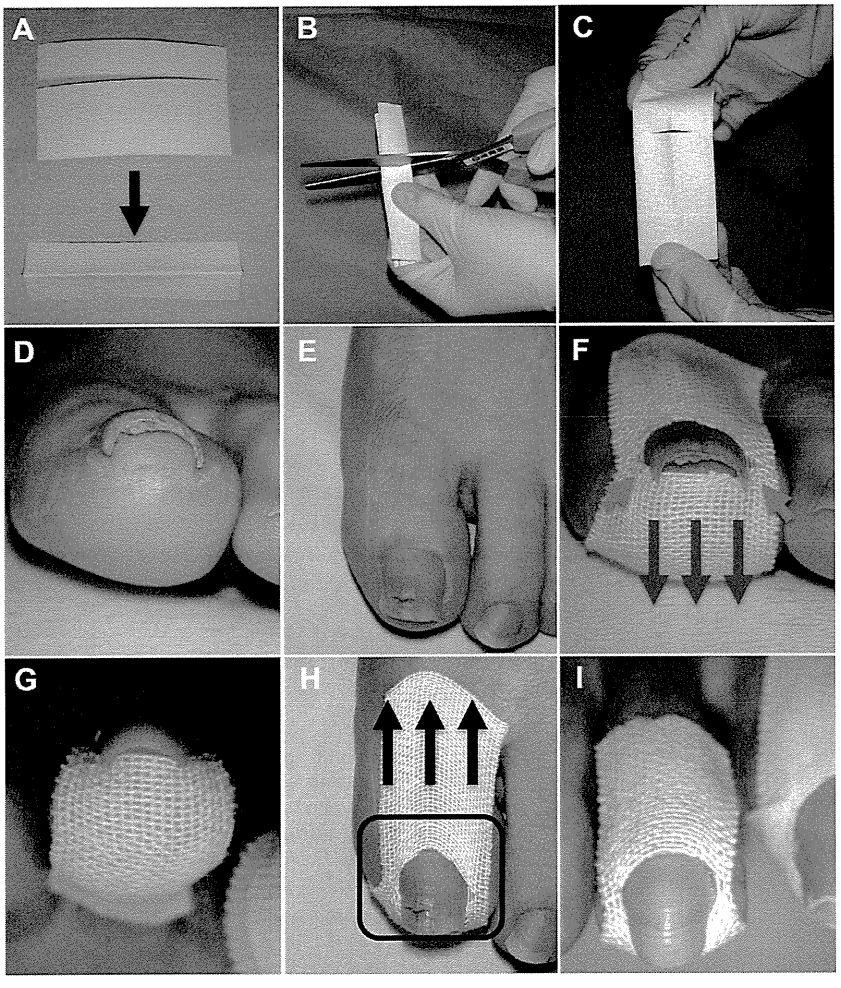

Fig. 1. Treatment modality of the "slit tape-strap" procedure. (A) Elastic tape is cut into pieces approximately 3 cm wide and 8–10 cm long and folded in half longitudinally. (B, C) A slit is cut at one-third the length of the tape-strap from the short edge. (D, E) Clinical presentation of ingrown toenail on the left foot. (F) The ingrown nail tip is set in the centre of slit with the shorter side of the tape oriented toward the dorsal side of the toe. The edge of the slit is hooked on the edge of the ingrown nail (*red arrows*). The shorter side of the tape is attached to the dorsal side of the toe, while the longer side of the tape-strap is attached to the plantar side of the toe under tension in order to draw the nail-fold skin toward the plantar side (*blue arrows*). (G) The edge of the slit beneath the ingrown toenail. (H) The shorter side of the tape is stretched to attach to the dorsal side of the toe (*black arrows*) in order that the slit in the tape is hooked between the free nail edge and the nail bed. (I) The "slit tape-strap" procedure is applied to the second toe with the tape adjusted to an appropriate width.

RESULTS

Patients' characteristics and procedures

We retrospectively reviewed 140 ingrown toenails of 121 patients in total (mean ± standard deviation (SD): age 54.6 ± 19.1 years; median and range: 58 and 7–92 years, respectively). The sample comprised 103 toenails from female patients and 37 nails from male patients. Among them, 50 ingrown toenails were either infected with fungi, as confirmed by KOH examination, or accompanied by bacterial paronychia with pus discharge.

We treated 140 ingrown toenails with 6 different procedures (Table I). Thirty-eight cases were treated with monotherapy of the "split tape-strap" procedure (Procedure 1) (Fig. 1), 31 cases with the "split tape-strap" procedure + elastic wire device (Procedure 2) (Fig. S1D[1]), 20 with the "split tape-strap" procedure + gutter method (Procedure 3) (Fig. S1C[1]), 12 cases with the "split tape-strap" procedure + a shape-memory alloy (Procedure 4) (Fig. S1F[1]), 10 cases with the "split tape-strap" procedure + Nishioka's procedure (Procedure 5) (Fig. S1A and B[1]), and 29 cases with various combinations of more than 2 different treatments (Procedure 6). Most of the patients visited every 2 weeks for the first 2 months and then every month thereafter.

This study included 45 toenails of clinical type 1, 43 of type 2, 41 of type 3, and 11 of type 4. Procedure 1 was performed for 4 toenail types, with higher frequency for type 3. Procedure 2 was performed with higher frequency for type 2. Procedure 3 was mainly for ingrown toenails accompanied by excessive granulation tissue. Procedures 4 and 5 were used for fewer cases of type 2. Procedure 6 was used for more cases of type 2. All procedures relieved pain for a mean of 3.7–6.8 days after the initiation of treatment. The mean duration required to completely cure an ingrown toenail ranged from 17.6 to 25.1 weeks. Patients treated with procedures 1 and 6 showed earlier resolution until cure of the ingrown toenail, while those treated with Procedure 2 required more time for complete resolution. Among these cases, however, 18 cases recurred 3 or more months after they were completely cured. The recurrence rates vary from 0% to 25% depending on the treatment modalities.

Tape-strap method combined with operative and other conservative treatments

One of the benefits of the "slit tape-strap" procedure is that it is able to support other conventional and surgical treatments. Nishioka's procedure is also useful for drawing the granulation tissue away from an ingrowing toenail, but tape alone often fails to draw it away sufficiently because of the wet surface. The "slit tape-strap" procedure can be used as the anchor tape of Nishioka's procedure in order to cover the wet surface of the granulation tissue with elastic tape (Fig. S1A and B[1]). Because the "slit tape-strap" covers wet granulation tissues, tapes of Nishioka's procedure can adhere rigidly to the anchoring "slit tape-strap" and can efficiently draw granulation tissue away from the edge of nails. Furthermore, it is useful with the gutter method to keep the splinting tube away from the granulation tissue (Fig. S1C[1]). This procedure protects the nail bed or nail fold from injury and contact with the metal devices when elastic wire devices, VHO-Osthold brace, or shape-memory alloy devices are applied (Fig. S1D–F[1]). After cutting the edge of a pincer toenail, it prevents the growing nail from hurting the nail bed and edge (Fig. S1G–I[1]). Thus the "slit tape-strap" procedure is useful as a supportive treatment for other methods.

[1]http://www.medicaljournals.se/acta/content/?doi=10.2340/00015555-2065

Table I. *Demographic data and treatment outcomes of each treatment procedure for ingrown toenails*

No.	Procedures	Ingrown toenails *n*	Sex, F/M *n*	Age, years Mean ± SD Median (range)	Involved toes First *n*	Involved toes Others *n*	Clinical types of nail shapes[a] 1 *n*	2 *n*	3 *n*	4 *n*	Excessive granulation *n* (%)	Infection[b] *n* (%)	Duration until pain relief, days Mean ± SD Median (range)	Duration until cure of ingrown toenail, weeks Mean ± SD Median (range)	Recurrence *n* (%)
1	Slit tape-strap (STS)	38	28/10	57.1 ± 17.3 59.5 (23–90)	34	4	10	8	18	2	2 (5)	15 (3)	3.7 ± 4.0 2.0 (0.3–16)	17.6 ± 10.3 13.5 (5–36)	3 (8)
2	STS + Elastic wire	31	26/5	58.0 ± 18.1 62.0 (14–92)	31	0	12	15	4	0	1 (3)	7 (23)	6.8 ± 5.5 6.0 (0.4–24)	25.1 ± 11.4 24.0 (7–48)	5 (16)
3	STS + Gutter	20	10/10	43.1 ± 25.1 42.0 (7–81)	17	3	6	2	5	7	19 (9)	14 (7)	4.5 ± 5.4 2.5 (0–24)	20.3 ± 11.5 17.5 (7–52)	1 (5)
4	STS + Shape-memory alloy	12	11/1	54.8 ± 16.6 55.5 (30–74)	12	0	5	2	5	0	0 (0)	4 (33)	3.9 ± 2.3 3.5 (1–8)	19.9 ± 10.3 20.0 (5–44)	3 (25)
5	STS + Nishioka's procedure	10	5/5	61.7 ± 20.8 61.5 (21–86)	10	0	3	1	4	2	4 (4)	3 (30)	5.1 ± 7.1 2.5 (0.3–24)	19.3 ± 13.9 15.5 (4–56)	0 (0)
6	STS + Multiple	29	23/6	53.1 ± 16.0 58.0 (20–84)	29	0	9	15	5	0	12 (41)	7 (24)	4.4 ± 3.8 3.0 (1–14)	22.6 ± 10.6 20.0 (7–48)	6 (21)
	Total	140	103/37	54.6 ± 19.1 58.0 (7–92)	133	7	45	43	41	11	38 (27)	50 (36)	4.8 ± 4.7 3.0 (0–24)	21.0 ± 11.2 20.0 (4–56)	18 (13)

[a]See the Patients and Methods section. [b]Includes fungal or bacterial infection.

DISCUSSION

In general, ingrown toenails are treated either with operative or conservative treatments. Operative treatments for ingrowing toenails, such as nail avulsion and matricectomy, require equipment and skilled physicians, are often contraindicated by the patient's general condition or infection around the nail, and have the serious drawback of pain during and after the operation. Even with the proper procedures, operative treatments occasionally result in relapse of the ingrown toenail and nail deformity. In contrast, conservative treatments can be applied without equipment in a clinic or at home and induce fewer complications than operative treatment. Compared with operative therapies, however, conservative treatments take longer time to achieve satisfactory results because their success depends on proper nail growth. Thus, it is essential for conservative therapies to be easy and self-administrable by the patients themselves.

The taping method for ingrown toenails was first introduced by Nishioka et al. (6). The object of the method is to pull the lateral nail fold away from the offending lateral nail edge. Performed correctly and consistently, it can achieve its goal in mild cases of ingrown toenails. The technique of Nishioka's procedure is, however, crucial, and most patients require repeated education concerning how to perform it. Moreover, if the skin surrounding ingrown toenails is wet for any reason, it is difficult to apply this procedure because of the loss of adhesiveness of the elastic tape. To overcome this drawback, we devised the "slit tape-strap" procedure. Since, in this procedure, one edge of the slit is hooked on the edge of the ingrown toenail and the tape adheres to the skin throughout the whole circumference of the ingrown nail, a focal wet surface of the skin surrounding the ingrown toenail does not disturb this procedure.

Furthermore, this retrospective study revealed the following benefits of the "slit tape-strap" procedure: (*i*) it is convenient for patients of all ages regardless of their complications, (*ii*) it is effective for mild to severe ingrowing toenails, (*iii*) it can reduce downtime, (*iv*) it is useful as an anchor tape on granulation tissues, and (*v*) it can be combined with other methods. Any kind of elastic tape can be used for the tape-strap methods, and most elastic tapes are not expensive. Because patients can change the tape themselves, nails can be washed and the tape-strap can be changed easily. In our experience, all patients and families could follow this procedure after they were instructed once.

Recently, epidermal growth factor receptor (EGFR) inhibitors have become part of the therapeutic arsenal available for advanced colorectal cancer, non-small-cell lung cancer, pancreatic cancer and squamous-cell carcinoma of the head and neck. Paronychias are the earliest and most common form of ungual lesions, and are observed in 10–30% of patients receiving EGFR inhibitors (reviewed by Peuvrel et al. (11)). Paronychias can be complicated by excessive granulation (12). Although paronychias regress rapidly within a few days once treatment is discontinued (12, 13), the clinical course of excessive granulation tissue is prolonged, even following the withdrawal of EGFR inhibitors (14). For such cases, the "slit tape-strap" procedure is recommended.

In conclusion, this retrospective study shows that conservative treatment can cure most cases of ingrown toenails and that, depending on the circumstances, the novel "slit tape-strap" procedure provides an effective treatment modality as a monotherapy or in conjunction with other conservative therapies.

ACKNOWLEDGEMENTS

We thank Yumiko Ito for valuable technical support. This study was supported in part by the Global-COE Program from the Japanese Ministry of Education, Culture, Sports, Science and Technology.

The authors declare no conflicts of interests.

REFERENCES

1. Haneke E. Controversies in the treatment of ingrown nails. Dermatol Res Pract 2012; 2012: 783924.
2. Senapati A. Conservative outpatient management of ingrowing toenails. J R Soc Med 1986; 79: 339–340.
3. Wallace WA, Milne DD, Andrew T. Gutter treatment for ingrowing toenails. BMJ 1979; 2: 168–171.
4. Schulte KW, Neumann NJ, Ruzicka T. Surgical pearl: nail splinting by flexible tube – a new noninvasive treatment for ingrown toenails. J Am Acad Dermatol 1998; 39: 629–630.
5. Arai H, Arai T, Nakajima H, Haneke E. Formable acrylic treatment for ingrowing nail with gutter splint and sculptured nail. Int J Dermatol 2004; 43: 759–765.
6. Nishioka K, Katayama I, Kobayashi Y, Takijiri C. Taping for embedded toenails. Br J Dermatol 1985; 113: 246–247.
7. Machida E, Maruyama K, Sano S. [The correction of ingrown, curved nails with super elastic wire.] J Jpn Soc Surg Foot 1999; 20: S87 (in Japanese).
8. Moriue T, Yoneda K, Moriue J, Matsuoka Y, Nakai K, Yokoi I, et al. A simple therapeutic strategy with super elastic wire for ingrown toenails. Dermatol Surg 2008; 34: 1729–1732.
9. Ishibashi M, Tabata N, Suetake T, Omori T, Sutou Y, Kainuma R, et al. A simple method to treat an ingrowing toenail with a shape-memory alloy device. J Dermatolog Treat 2008; 19: 291–292.
10. Baran R, Haneke E, Richert B. Pincer nails: definition and surgical treatment. Dermatol Surg 2001; 27: 261–266.
11. Peuvrel L, Bachmeyer C, Reguiai Z, Bachet JB, Andre T, Bensadoun RJ, et al. Semiology of skin toxicity associated with epidermal growth factor receptor (EGFR) inhibitors. Support Care Cancer 2012; 20: 909–921.
12. Robert C, Soria JC, Spatz A, Le Cesne A, Malka D, Pautier P, et al. Cutaneous side-effects of kinase inhibitors and blocking antibodies. Lancet Oncol 2005; 6: 491–500.
13. Rigopoulos D, Larios G, Gregoriou S, Alevizos A. Acute and chronic paronychia. Am Fam Physician 2008; 77: 339–346.
14. Agero AL, Dusza SW, Benvenuto-Andrade C, Busam KJ, Myskowski P, Halpern AC. Dermatologic side effects associated with the epidermal growth factor receptor inhibitors. J Am Acad Dermatol 2006; 55: 657–670.

RESEARCH ARTICLE

Therapeutic Concentration of Lithium Stimulates Complement C3 Production in Dendritic Cells and Microglia via GSK-3 Inhibition

Zhiqian Yu,[1,2,3] Chiaki Ono,[1,2,3] Setsuya Aiba,[4] Yoshie Kikuchi,[1,2,3] Ichiro Sora,[2] Hiroo Matsuoka,[5] and Hiroaki Tomita[1,2,3]

Evidence indicates that widely prescribed mood stabilizer, lithium (Li), mediates cellular functions of differentiated monocytic cells, including microglial migration, monocyte-derived dendritic cell (MoDC) differentiation, and amelioration of monocytic malfunctions observed in neuropsychiatric diseases. Here, we surveyed molecules which take major roles in regulating these monocytic cellular functions. MoDCs treated with 1 and 5 mM Li, and microglia separated from Li-treated mice were subjected to microarray-based comprehensive gene expression analyses. Findings were validated using multiple experiments, including quantitative PCR, ELISA and immunostaining studies. Differing effects of Li on the two cell types were observed. Inflammation- and chemotaxis-relevant genes were significantly over-represented among Li-induced genes in MoDCs, whereas no specific category of genes was over-represented in microglia. The third component of complement (C3) was the only gene which was significantly induced by a therapeutic concentration of Li in both MoDCs and microglia. C3 production was increased by Li via GSK-3 inhibition. Li-induced C3 production was seen only in differentiated monocytic cells, but not in circulating monocytes. Our findings highlight a link between Li treatment and C3 production in differentiated monocytic cells, and reveal a regulatory role of GSK-3 in C3 production. Induction of microglial C3 production might be a novel neuroprotective mechanism of Li via regulating interactions between microglia and neurons.

GLIA 2015;63:257–270

Key words: mood stabilizer, complement component 3, glia cell, monocytic cells, psoriasis

Introduction

Lithium (Li) is a commonly prescribed mood stabilizer that reduces and prevents manic and depressive symptoms of bipolar disorder (BD). Among the various effects attributed to Li, its inhibitory effect on glycogen synthase kinase-3 (GSK-3) is considered the major mechanism of its mood stabilizing action. Although most studies relating to the mechanism of action of Li have focused on neurons, astrocytes and oligocytes (Azim and Butt, 2011; Li et al., 2002; Yu et al., 2011), recent studies point to a role for Li in inhibiting GSK-3 in immune cells, including lymphocytes (Beurel, 2011), monocytic cells such as peripheral monocytes (Martin et al., 2005), macrophages (Park et al., 2011), monocyte-derived dendritic cells (MoDCs) (Rodionova et al., 2007), and microglia (Yuskaitis and Jope, 2009). For example, GSK-3 has been shown to regulate cytokine production by T cells and the differentiation of T cells into specific subtypes, particularly T_H17 cells (Beurel et al., 2011). GSK3 promotes the production of pro-inflammatory cytokines, such as interleukin-6 (IL-6), IL-12, IL-1β, and tumor necrosis factor-α (TNF-α) in

View this article online at wileyonlinelibrary.com. DOI: 10.1002/glia.22749

Published online September 1, 2014 in Wiley Online Library (wileyonlinelibrary.com). Received Oct 25, 2013, Accepted for publication Aug 15, 2014.

Address correspondence to Hiroaki Tomita, Department of Disaster Psychiatry, International Research Institute for Disaster Science, Tohoku University, 4-1 Seiryo-machi, Aoba-ku, Sendai, 980-8574, Japan. E-mail: htomita@med.tohoku.ac.jp

From the [1]Department of Disaster Psychiatry, International Research Institute for Disaster Science, Tohoku University, Sendai, Japan; [2]Department of Biological Psychiatry, Graduate School of Medicine, Tohoku University, Sendai, Japan; [3]Tohoku Medical Megabank Organization, Tohoku University, Sendai, Japan; [4]Department of Dermatology, Graduate School of Medicine, Tohoku University, Sendai, Japan; [5]Department of Psychiatry, Graduate School of Medicine, Tohoku University, Sendai, Japan.

Additional Supporting Information may be found in the online version of this article.

human monocytic cells (Martin et al., 2005), whereas its inhibition increases the production of anti-inflammatory cytokines, such as IL-10, in human monocytic cells (Martin et al., 2005) and primary rat microglia (Huang et al., 2009).

Some evidence points to the possibility that immunological mechanisms may be involved in the pathophysiology of BD, and that Li may exert its effects, at least in part, by acting on central and/or peripheral monocytic cells. Postmortem brain studies revealed that inflammatory markers, including IL-1 and IL-1R, were elevated in the frontal cortices of BD patients (Rao et al., 2010). BD patients also show phasic alterations in cytokine levels in blood (Kim et al., 2007), plasma and serum (Munkholm et al., 2013). IL-10, soluble inlerleukin-2 receptor (sIL-2R) and TNF-α levels are increased in BD patients (Modabbernia et al., 2013; Munkholm et al., 2013), and among BD patients, manic or depressive patients showed higher TNF-α levels compared with euthymic patients (Kim et al., 2007; Ortiz-Dominguez et al., 2007). Levels of IL-1, IL-2, IL-4, IL-6 and soluble tumor necrosis factor receptor type 1 are also reportedly altered in BD patients (Kim et al., 2007; Ortiz-Dominguez et al., 2007).

Monocytic cell function is also altered in BD patients. For example, monocytes isolated from BD patients are hampered in their ability to differentiate into MoDCs and weakly stimulate autologous T cells; these effects are abolished by Li treatment (Knijff et al., 2006). Among immune cells, differentiated monocytic cells, such as dendritic cells and microglia, play pivotal roles in the innate immune system in both the brain and peripheral tissues via their migratory and phagocytic functions, or by releasing cytokines and complement components (Austyn, 1996; Banchereau et al., 2000; Becher et al., 2000; Gasque et al., 2000; Hanisch, 2002).

Taken together, studies on Li suggest that it may exert its effects, at least in part, by acting on peripheral and/or central differentiated monocytic cells. Although it is interesting to assess the functional changes of microglia in the human brain after Li treatment, there is a technical restriction. On the other hand, MoDCs can be obtained from peripheral blood samples. Because microglia and dendritic cells share the same phylogenic origin (Santambrogio et al., 2001) and similar morphological and physiological characteristics (Bulloch et al., 2008; Fischer and Reichmann, 2001; Santambrogio et al., 2001), it is expected that phenomena observed in MoDCs may at least in part reflect phenomena in microglia. In a wider scope, our hypothesis is that peripheral biomarkers are present in human MoDCs and reflect the functional changes of brain microglia after Li treatment because of the similarity between DC and microglia. To initiate this investigation, we conducted microarray-based gene expression analyses on Li-treated human MoDCs and mouse microglia, to identify similar changes in their gene expression profiles. Gene expression profiles of Li-treated human MoDCs and mouse microglia are quite different, which is contrary to our hypothesis that they may be similar. Although we failed to find a set of genes that are similarly altered in both Li-treated human MoDCs and mice microglia, we found a gene that showed outstanding expression profiling in terms of common alterations in both monocytic cells. C3 was the only exception and showed significant elevation after administration of a therapeutic concentration of Li in both human MoDCs and mouse microglia.

Materials and Methods

Culturing of Human Monocyte-Derived Dendritic Cells (MoDCs) and Monocyte-Derived Macrophages (MDMs)

$CD14^+$ monocytes were separated from peripheral blood mononuclear cells from eight healthy volunteers using CD14 MicroBeads and a magnetic cell separator (Miltenyi Biotec, Bergisch Gladbach, Germany). Purity of $CD14^+$ cells (>98%) was confirmed using FACSCalibur (BD Bioscience, Mountain View, CA) with fluorescein-labeled anti-CD14 antibody (BD Bioscience). For MoDCs differentiation studies, $CD14^+$ monocytes (2×10^6) were cultured in six-well plates containing 1 mL of RPMI 1640 medium (BioWhitaker, Walkersville, MD) with 10% fetal bovine serum, 50 ng/mL GM-CSF (Peprotech EC, London, UK) and 100 ng/mL interleukin 4 (Peprotech EC) (Knijff et al., 2006), with or without lithium chloride (Li) (Kanto chemical Co., Tokyo, Japan) for 6 days. MDMs were differentiated in medium containing 50 ng/ml GM-CSF (Peprotech EC), 100 ng/mL M-CSF (Peprotech EC) and 30 ng/ml interleukin 3 (Peprotech EC) (Young et al., 1990), with or without Li for 6 days. Li concentrations were set at 1 mM (therapeutic concentration (Timmer and Sands, 1999)) or 5 mM (lethal concentration (Dawson and Whyte, 1999), although often used to potently inhibit GSK-3 in *in vitro* studies). Every 3 days, half of the medium was replaced with fresh medium. After 3 and 6 days, medium was collected and stored at −20°C and subjected to the following studies. To investigate the effect of an alternative GSK-3 inhibitory agent on monocytic cells, the GSK-3 inhibitor, SB-216763, was added to medium in place of Li at concentrations of 20 nM or 100 nM. These concentrations show GSK-3 inhibitory potencies equivalent to 1 mM or 5 mM of Li, respectively (Coghlan et al., 2000; Klein and Melton, 1996). Since SB-216763 is water-insoluble, the agents were first dissolved in dimethyl sulfoxide (DMSO), and then added to medium (final DMSO concentration: 0.0001%). Control MoDCs were cultured in media containing the same concentration of DMSO. Unless otherwise indicated, chemicals were purchased from Sigma-Aldrich (St. Louis, MO).

Culturing of Mouse Cell Lines

The mouse microglia cell line, MG-6 (RIKEN Cell Bank, Tsukuba, Japan), and mouse monocyte-like cell line, WEHI-274.1 (ATCC, Manassas, VA), which were cultured in DMEM medium (Wako

Pure Chemical Co., Osaka, Japan) containing 10% FBS, 10 μg/mL insulin and 100 μM 2-mercaptoethanol, were subjected to Li or SB-216763 treatment in the same manner as described for the MoDCs experiments. The mouse macrophage-like cell line, J774.1 (RIKEN Cell Bank), was cultured in RPMI 1640 medium (Wako Pure Chemical) containing 10% FBS with or without Li for 6 days. For all cell lines, 2×10^6 cells were cultured in 1 mL of medium in six-well plates.

Experimental Animals and Drug Treatment

Animals were individually housed and maintained on a 12:12 light/dark schedule with *ad libitum* access to food and water throughout the course of the entire experiment. Experimental protocol was approved by the Institutional Animal Care and Use Committee of Tohoku University. Sixty male C57BL/6 mice (SLC Japan Inc., Shizuoka, Japan) weighing 20 to 30 g were divided into six groups. Three of the six groups were given Li-containing water (600 mg/L) for 2 weeks, while the remaining three groups were given tap water during the same period. No profound changes in appearance or behavior were observed in these mice, whereas severe decreases in food intake and body weight were observed in mice fed with higher Li concentrations in a preliminary study. After sacrificing the mice, whole brains were dissociated into single-cell suspensions using the Neural Tissue Dissociation Kit and a gentleMACS Dissociator (Miltenyi Biotec). This was followed by isolation of CD11b-positive microglia with CD11b MicroBeads and a magnetic cell separator (Miltenyi Biotec). Likewise, Mac-1 (CD11b/CD18)-positive monocytes were isolated from blood mononuclear cells using Mac-1 MicroBeads (Wong et al., 2006). Purity of $CD11b^+$ cells (>98%) was confirmed using FACSCalibur (BD Bioscience) with fluorescein-labeled anti-CD11b antibody (BD Bioscience). Serum was used to confirm Li concentrations (0.38 ± 0.01 mEq/L). Ten isolated microglia samples from each group were pooled, and six pooled samples (three from Li-treated mice, three from control mice) were subjected to microarray experiments.

Microarray Experiments and Data Analysis

RNA extraction and microarray experiments were performed as previously described (Yu et al., 2011). Equal aliquots of MoDCs from eight individuals were added to three flasks and incubated in medium containing 0 mM, 1 mM, or 5 mM Li. Total RNA was extracted from the 24 MoDCs samples (for three types of medium × eight individuals) were applied to 24 Human-6v2 BeadChip microarrays. Microglia samples were isolated from 10 mice from each of the six groups; three groups were treated with Li and the remaining three groups were given tap water, and the samples were pooled for each group. Total RNA was extracted from the six pooled samples (three Li-treated microglia samples and three controls) and applied to six MouseWG-6v2 BeadChip microarrays. The inter-array variation among the 24 human microarrays or 6 mouse microarrays was normalized using average normalization after subtracting background signal intensities (SIs) using Illumina BeadStudio 3.1 software (Illumina). To screen for candidate genes, SIs of total probe sets for subjects treated with Li were compared with those for non-treated subjects. Based on mean SIs from the microarray data, transcripts with SIs of greater than 100 were considered reliably detectable. Over-representation was analyzed using the Database for Annotation, Visualization and Integrated Discovery (DAVID) (http://www.david.abcc.ncifcrf.gov) (Dennis et al., 2003).

Quantitative Real-Time PCR

Total RNA was extracted and subjected to cDNA synthesis with random primers using the SuperScript VILO cDNA synthesis kit (Invitrogen, Carlsbad, CA). The relative copy number of each transcript in each cDNA sample was measured using specific primers and the iQ SYBR Green Supermix (Bio-Rad Inc., Hercules, CA) with a CFX96 real-time PCR detection system (Bio-Rad). Target genes were selected based on the microarray data, and human or mouse glyceraldehyde-3-phosphate dehydrogenase (*GAPDH* or *Gapdh*) and 18S rRNA (data not shown) were used as internal controls for normalization. Forward and reverse primers for human *C3* were 5′-ATCATCGGGAAGGACACTTG-3′ and 5′-TTATCTGGAGTGGGGGAATG-3′, respectively. Forward and reverse primers for mouse *C3* were 5′-ATCAGCCACATCAAGTGCAG-3′ and 5′-CTGTGAATGCCCCAAGTTCT-3′, respectively. Forward and reverse primers for human *GAPDH* were 5′-GTCAGTGGTGGACCTGACCT-3′ and 5′-TGCTGTAGCCAAATTCGTTG-3′, respectively. Forward and reverse primers for mouse *Gapdh* were 5′-GAGGACCAGGTTGTCTCCTG-3′ and 5′-ATGTAGGCCATGAGGTCCAC-3′, respectively. Forward and reverse primers for human 18_S rRNA were 5′-GAACGAGACTCTGGCATGCTAA-3′ and 5′-CTCAATCTCGGGTGGCTGAA-3′, respectively. Forward and reverse primers for mouse 18_S rRNA were 5′- GTAACCCGTTGAACCCCATT-3′ and 5′-CCATCCAATCGGTAGTAGCG-3′, respectively. Forward and reverse primers for human *MMP9* were 5′-GAGTTCCCGGAGTGAGTTGA-3′ and 5′-ACTCCTCCCTTTCCTCCAGA-3′, respectively. Forward and reverse primers for mouse *Mmp9* were 5′-AACACCACCGAGCTATCCAC-3′ and 5′-AGGAGTCTGGGGTCTGGTTT-3′, respectively. Forward and reverse primers for human *S100A9* were 5′-TAAGACCACAGTGGCCAAGA-3′ and 5′-CCACAGCCAAGACAGTTTGA-3′, respectively. Forward and reverse primers for mouse *S100a9* were 5′-GATGCTGATGGCAAAGTTGA-3′ and 5′-GCCATTGAGTAAGCCATTCC-3′, respectively. A standard curve was constructed for each assay to adjust for differences in the amplification efficiency between primer sets.

ELISA Measurements of Secreted C3 in Cell Culture Medium and Mouse Serum

C3 levels in medium from cultures of human MoDCs and MDMs were measured using the human C3 ELISA quantitation kit (GenWay Biotech, San Diego, CA), whereas C3 in mouse cell line culture medium and mouse serum were measured by sandwich ELISA, using a goat anti-mouse C3 antibody (1:500; MP Biomedicals, Aurora, OH) and HRP-conjugated goat anti-mouse C3 antibody (1:1,000; MP Biomedicals). Mouse C3 reference serum (Alpha Diagnostic Intl., San Antonio, TX) was used to generate a standard curve. Optical density at 405 nm was measured with a SpectraMAX 190 Microplate Reader (Molecular Devices).

Immunostaining of Mouse Microglia

To determine the effect of Li on C3 expression in mouse microglia *in vivo*, mice were treated with or without Li (n = 6, each) for 2 weeks in the same manner as the animal experiments described above. Hippocampal slices (10 μm thick) dissected from frozen brains were stained with goat anti-mouse complement C3 (1:500; MP Biomedicals) and rat anti-mouse CD11b (1:1,000; AbD Serotec, Oxford, UK) antibodies, along with the following secondary antibodies: Alexa Fluor 488 anti-rat IgG and Alex Fluor 594 anti-goat IgG (1:300; Invitrogen). 4, 6-diamidino-2-phenylindole (DAPI) (Invitrogen) was used for nuclear staining. Microscopic images were captured using a Leica DAS Mikroskop microscope (Leica Microsystems, Wetzlar, Germany). Results were quantified using ImageJ 1.42 software.

Fluorescence-Activated Cell Sorting of MoDCs

Cells were incubated with anti-human FITC- or PE (phycoerythrin)-conjugated monoclonal antibodies (mAbs) to evaluate the characteristics of Li-treated MoDCs. Cell death was assessed with propidium iodide (PI). The following mAbs were used for flow cytometry: PE-conjugated anti-CD14 antibody (Beckman Coulter, Krefeld, Germany), PE-conjugated anti-CD1a antibody (Beckman Coulter) and FITC-conjugated anti-CD86 antibody (BD Pharmingen, San Diego, CA). FITC-conjugated anti-IgG1 (BD Pharmingen) and PE-conjugated anti-IgG1 (BD Pharmingen) were used as negative controls. After mAb staining, cells were subjected to flow cytometry with a BD FACSCalibur (BD Pharmingen) cell sorter and analyzed using CellQuestPro software (BD Pharmingen).

Western Blot Analysis

Supernatants of homogenized MG-6 cells were subjected to sodium dodecyl sulfate polyacrylamide gel electrophoresis, followed by transferring to membranes. Membranes were probed with a goat polyclonal anti-GAPDH antibody (1:1,000; Abcam, Cambridge, UK), monoclonal anti-β-actin antibody (1:10,000) or mouse monoclonal β-catenin antibody (1:1,000; Abcam). The secondary antibody was a peroxidase-conjugated goat anti-mouse IgG antibody (1:5,000; Jackson ImmunoResearch, West Grove, PA). Chemiluminescence was detected using an Amersham ECL Plus western blotting detection kit (GE Healthcare, Piscataway, NJ) and a LAS-1000 luminescence image analyzer (Fujifilm, Tokyo, Japan), and quantified using ImageJ 1.42 software (http://rsb.info.nih.gov/ij/).

Phagocytosis Assay

Phagocytosis was assessed with the CytoSelect 96-well phagocytosis assay (Cell Biolabs Inc., San Diego, CA) and sheep erythrocytes (Nippon Biotest Laboratories Inc., Tokyo, Japan). The amount of engulfed erythrocytes was determined with a colorimetric assay using a SpectraMAX 190 Microplate Reader (Molecular Devices, Sunnyvale, CA).

Statistical Analysis

Differentially expressed genes in the microarray data of human MoDCs were analyzed using one-way repeated measure ANOVA followed by Fisher's least significant difference *post hoc* test (GeneSpring GX 10.0; Agilent Technologies, Santa Clara, CA). A two-tailed unpaired Student's t-test was used to examine differences in mean values between groups in the *in vivo* studies and western blot analysis. One-way ANOVA followed by Dunnett's *post hoc* test was used for the other studies. Statistical analysis was performed with GraphPad Prism version 6 (GraphPad Software, San Diego, CA).

Results

Microarray Gene Expression Profiles of Human MoDCs and Mouse Microglia

We initially evaluated the effects of therapeutic (1 mM) and high (5mM) concentrations of Li on human MoDCs RNA expression. Among the 48,701 transcripts on the microarray, 9,714 with signal intensities (SIs) greater than 100 in all 24 MoDCs samples assessed were considered reliably detectable. Among the reliably detectable genes, 78 genes and 382 genes were significantly increased by 1 mM- and 5 mM-Li treatment, respectively, based on the criteria: P value of one-way repeated measures ANOVA followed by Fisher's least significant difference *post hoc* test of less than 0.05, and fold change (FC) of greater than 1.2 compared to controls. Likewise, 146 genes and 651 genes were significantly decreased by 1 mM- and 5 mM-Li treatment, respectively, based on the criteria: P of less than 0.05 and FC of less than 0.833. Among these significantly altered genes, 49 genes showed increased SIs in a concentration-dependent manner based on the following criteria: average SI of 5 mM Li-treated MoDCs was at least 20% higher than the average SI of 1 mM Li-treated MoDCs and the average SI of 1 mM Li-treated MoDCs was at least 20% higher than the average SI of 0-mM Li-treated MoDCs. Similarly, 92 genes showed decreased SIs in a concentration-dependent manner based on the following criteria: average SI of 5-mM Li-treated MoDCs was at least 20% lower than the average SI of 1-mM Li-treated MoDCs and the average SI of 1-mM Li-treated MoDCs was at least 20% lower than the average SI of 0-mM Li-treated MoDCs. Gene symbols, Probe ID, and Gene accession ID for the 10 genes showing the most robust increases and decreases in MoDCs are listed in Table 1. For mouse microglia, among the 45,821 transcripts on the microarray, 10,983 were considered reliably detectable in all six mouse microglia samples treated with or without Li. Among these detectable genes, levels of 104 genes were increased with a FC of greater than 1.2 by Li treatment, whereas levels of 126 genes were decreased with a FC of less than 0.833. Gene symbols, Probe ID, and Gene accession ID for the 10 genes showing the most robust increases and decreases in MoDCs are listed in Table 1.

The effects of a therapeutic concentration of Li on the gene expression profiles of human MoDCs and mouse microglia substantially differed. Based on DAVID analyses (Bonferroni correction for multiple category comparisons, $P < 0.05$), "inflammation" and "chemotaxis" were the two biological processes in which Li-induced genes were significantly